Utkarsha L. Mohite* and Hirenkumar G. Patel

Robust controller for cancer chemotherapy dosage using nonlinear kernel-based error function

https://doi.org/10.1515/bams-2019-0056
Received October 30, 2019; accepted August 31, 2020;
published online September 28, 2020

Abstract: It is well-known that chemotherapy is the most significant method on curing the most death-causing disease like cancer. These days, the use of controller-based approach for finding the optimal rate of drug injection throughout the treatment has increased a lot. Under these circumstances, this paper establishes a novel robust controller that influences the drug dosage along with parameter estimation. A new nonlinear error function-based extended Kalman filter (EKF) with improved scaling factor (NEF-EKF-ISF) is introduced in this research work. In fact, in the traditional schemes, the error is computed using the conventional difference function and it is deployed for the updating process of EKF. In our previous work, it has been converted to the nonlinear error function. Here, the updating process is based on the prior error function, though scaled to a nonlinear environment. In addition, a scaling factor is introduced here, which considers the historical error improvement, for the updating process. Finally, the performance of the proposed controller is evaluated over other traditional approaches, which implies the appropriate impact of drug dosage injection on normal, immune and tumor cells. Moreover, it is observed that the proposed NEF-EKF-ISF has the ability to evaluate the tumor cells with a better accuracy rate.

Keywords: chemotherapy; controller; drug dosage; error function; extended Kalman filter.

Introduction

As cancer is turning out be a dreadful disease [1–3], it is necessary to improve the diagnostic benefits of the treatment. Moreover, it is significant to compute the efficiency of the chemotherapy plan and its viability. In fact, chemotherapy [4–6] is a traditional technique that is used for treating cancer in medical practice [37–40]. The deliverance of chemotherapy drugs is found to be a better therapeutic approach and it has attained a worldwide consideration these days. Nowadays, engineering science has contributed a lot to this research by formulating several numerical designs, which demonstrates the impact of chemotherapeutic drugs [7–9] and its dose.

These approaches were extensively deployed to develop and analyze a variety of drug controlling techniques [10–12]. These in "silico trials" are cost-efficient and it assists engineers and clinicians to analyze the consistency of new approaches for drug dosage in medical pharmacology. Nowadays, the combined usage of siRNAs and chemotherapy drugs [13, 14] remains a better treatment for cancer and it has gained much attention. The 2D-based models of siRNA and chemotherapy drug [15, 16] intend to minimize the side effects of the drugs and it also minimizes the adverse harms occurring to normal cells. On the other hand, after repetitive chemotherapy [17, 18], the severe undesirable effects resulting from chemo agents weaken the outcome, thus resulting in diagnostic failure [19–21, 41, 42].

In addition, Kalman filtering techniques play an essential role in estimating the dynamic states and it enhances the estimation accuracy. It also improves the precision and temporal resolution, thus ensuring a better estimation of the drug dosage levels [22–24]. However, a major issue in exploiting Kalman filter lies in setting up the covariance matrixes. Therefore, EKF is introduced that enhances the accuracy of dynamic state estimation. In addition, EKF could be applied for estimating the immune cells, and it can adjust the dosage of drugs and thus control the normal, immune and tumor cells in chemotherapy [25].

The major contribution of this paper is depicted below.

(1) This paper intends to present a novel robust controller that influences the drug dosage together with parameter estimation.
(2) Here, a novel NEF-EKF-ISF is introduced and the updating process is done depending on the prior error function, though scaled to a nonlinear environment.

***Corresponding author: Utkarsha L. Mohite**, Assistant Professor, Department of Electrical Engineering, SVNIT, Surat, India, E-mail: utkarshalmohite@gmail.com
Hirenkumar G. Patel, Department of Electrical Engineering, SVNIT, Surat, India

(3) Further, a scaling factor is established that considers the historical error enhancement for the updating process.
(4) Finally, the performance of the implemented controller is compared over other traditional schemes that demonstrate the impact of drug dosage injection on normal, immune and tumor cells.

The overall organization of the work is as follows: Section 2 portrays the review of the work. Section 3 describes the chemotherapy: nonlinear mathematical formulation. Section 4 presents the modeling of the robust adaptive control system and Section 5 portrays the enhanced Kalman filter with improved nonlinear kernel-based error function with scaling factor. Section 6 portrays the experimental outcomes, and Section 7 concludes the paper.

Literature review

Related works

In 2017, Regina et al. [1] have established a new method that insists on the necessity of carrying out cancer chemotherapy properly so that safe and effective treatment could be ensured. The majority of the approaches developed for scheduling cancer chemotherapy were model-oriented. Here, an RL-based technique was presented for regulating the dosage of chemotherapy drugs. Moreover, for optimal control of drug dosing, the Q-learning scheme was exploited. Finally, mathematical models were offered that have illustrated the performance of the adopted controller.

In 2019, Lai and Avner [2] have considered a combination of anti-VEGF and docetaxel for treating cancer. As anti-VEGF minimized the penetration of chemotherapy drugs, the issue comes up if it was much effectual for managing the two drugs together, so as to minimize the volume of tumor in an effective manner. For clarifying this issue, an arithmetical model was developed and deployed, by which various schedules were simulated. From the analysis, it was discovered that the diagnosis of cancer could be much better if the two drugs were taken in a non-overlapping manner, with the anti-VEGF for 21 days and chemotherapy drugs on day 0.

In 2018, Wu and Qiaodan [3] have formulated a model, where the issues in drug therapy were designed as an optimal problem of switched systems. It was varied from the conventional switching control systems, where the modes were switched based on time. Therefore, the conventional optimal controlling schemes based on time cannot be deployed for solving this issue directly, and hence a novel arithmetical evaluation scheme was developed for resolving these issues. At last, an arithmetical model was exploited that showed that the adopted model has rapid convergence speed and it has consumed less time when evaluated over the existing schemes.

In 2018, Liang et al. [4] have presented an effective model, which analyzed the effect of "autophagy protein p62" in OSCC cells after and before chemotherapy. Moreover, CAFs were recognized in these OSCC samples that explored the roles of CAFs and p62 in chemotherapy. In addition, the associations among clinical outcomes, expression of proteins and pathological features were examined, and the attained outcomes proposed that chemotherapy has raised the level of CAFs in OSCC.

In 2019, Khalili and Ramin [5] have presented a scheme, where the optimal controlling signals were attained via the steepest descent technique. Here, the solution's logic was evaluated with investigational outcomes. Subsequently, an adaptive controller, which considered the optimal path directed the system toward it. Further, "Barbalat lemma and Lyapunov stability theory" were deployed that have attained the stability of the closed-loop system. In addition, an online recursive estimation technique was exploited that have estimated certain parameters. Finally, the experimental outcomes pointed out the efficiency and performance of the modeled controller.

In 2019, Wang et al. [6] have introduced an effective combination chemotherapy schedule, which has determined the drug dosage given to cancer patients with drug resistance that might worsen the effectiveness of chemotherapy. For characterizing the growth of cells, the "cell cycle-specific" approach was exploited, which included the mechanism of attained drug resistance. To prevail over the complexity in discovering a suitable solution to this issue, MA was developed. Further, the effectiveness of the introduced model was confirmed by evaluating existing schemes.

In 2016, Nazila and Lotfi [7] have developed a new approach that dealt with the modeling of novel clinical trials for gastroesophageal and gastric cancers, and this scheme has discovered the cost-effective and optimal chemotherapeutic treatment model. Initially, data were extracted from the earlier clinical trials and then statistical models were developed, by which the trial outcomes were predicted. Then by using these arithmetical approaches, a multi-objective scheme was presented for planning the chemotherapeutic treatment. Finally, the outcomes demonstrated that the adopted model required only reduced cost and time when compared to the trial and error model.

In 2016, Sofiane et al. [8] have suggested an effective measurement-oriented controlling model for cancer

chemotherapy. Here, a two-degree-of-freedom PID controlling approach was presented for controlling the growth of cancer. These PID controllers offered the desired quantity of drug dosage to be provided into the body of patients by concerning the level of toxicity within their mentioned limits. The feasibility of the adopted cancer controlling scheme was further confirmed by an example in this work. Thus, the capability of the adopted controller was proved from the simulation outcomes.

In 2018, Hajar Nasiri and Ali Akbarzadeh Kalat [29] developed an intelligent controller for MIMO cancer immunotherapy system. The main objective was to attain an appropriate scheduling method for drug dosage to reduce the tumor cells. An adaptive fuzzy back-stepping controller for the MIMO cancer immunotherapy system was developed using the back-stepping approach as well as property of universal approximation of the fuzzy systems.

In 2019, Mojtaba Sharifi and Hamed Moradi [30], developed a novel composite adaptive control scheme for both of the minimizaion of cancer tumor volume and the online identification oftumor parameters at the time of the drug delivery process in chemotherapy. This control scheme was exploited for three different nonlinear mathematical cell-kill models of the cancer tumor.

In 2018, Francisco F. Teles and João M. Lemos [31], worked on a control system which models an optimal therapy on the basis of the adaptive control methods, aspiring to permit the obliteration of a metastatic renal cell carcinoma as rapidly and economically as probable, and with lower related toxicity.

In 2019, Farouk Zouari et al. [32], studied the model of neuro-adaptive tracking control strategies for non-integer order non-square systems subject to time-varying output constraints and input nonlinearities. At first, the mean-value theorem was included, and then the original non-affine non-square system with actuator nonlinearities was converted into an equivalent affine square form.

In 2019, Farouk Zouari [33] worked on the neural adaptive control of drug dosage regimens in cancer treatment. The main aim of the treatment was to attain a suitable system for the drug dosage to minimize the tumor cells.

Review

Table 1 shows reviews on the cancer chemotherapy dosage systems. At first, the RL model was introduced in [1], which guarantees effective treatment and it does not need knowledge on system dynamics. However, it has to focus more on adaptive RL models. PDE was exploited in [2] that are more effective and it also decreases the volume of the tumor, but it requires consideration of combined therapies. In addition, a Gradient algorithm was deployed in [3] that offers rapid speed of convergence and it also offers reduced computational time. Anyhow, it does not include penalty terms. Likewise, the Spearman rank correlation scheme was exploited in [4], which evaluates the association among SMA and p62 expressions and it is a reliable approach. However, it has to analyze the association between cancer cells and CAFs. Also, the steepest descent method was employed in [5], which offers optimal cost function and it personalizes the drug injection; however, it has to focus more on the closed-loop control. MA was exploited in [6] that minimizes the tumor cells and it also offers improved sensitivity; anyhow, it needs to analyze the realistic diagnosis via implementation. Ridge regression scheme was implemented in [7], which offers reduced cost and it lessens the effort and time, but logical parameters have to be concentrated more. At last, the PID controller was suggested in [8] that minimizes the processing time and it also offers better accuracy. However, it has to focus on the processing of control design.

Chemotherapy: non-linear mathematical formulation

This work intends to develop a novel nonlinear control scheme that is very much robust against the parameter uncertainties. Here, the system's performance is evaluated by deploying the chemotherapy of the least order model. The adopted scheme involves the interaction of tumor cells with the normal and immune cells. Eq. (1)–(3) shows the nonlinear model, in which $ID(n)$, $T(n)$ and $D(n)$ signifies the count of immune, normal and tumor cells at a time n, correspondingly.

$$\vec{ID} = st + \frac{\rho ID \cdot T}{\alpha + T} - q_1 ID \cdot T - t_1 ID - y_1 u_1 ID \tag{1}$$

$$\vec{T} = ra_1 T(1 - c_1 T) - q_2 ID \cdot T - q_3 TD - y_2 u_2 T \tag{2}$$

$$\vec{D} = ra_2 D(1 - c_2 D) - q_4 TD - y_3 u_3 D \tag{3}$$

Here, the considered control inputs are drug injections. The effect of the chemotherapy drug is signified by $u_1(n)$, $u_2(n)$ and $u_3(n)$, respectively, and y_1, y_2 and y_3 denote the effect of chemotherapy on destroying the cell population. In Eq. (2), ra indicates the per capita growth rates. This model assumes a type of immune cell, which can reduce the tumor size by a kinetic process. In addition, the model includes immunity

Table 1: Features and challenges of cancer chemotherapy dosage models using various techniques.

Author [citation]	Adopted methodology	Features	Challenges
Regina et al. [1]	RL	– It guarantees effective treatment. – Do not need knowledge of system dynamics.	– Have to focus more on adaptive RL models.
Lai and Avner [2]	PDE model	– More effective. – It decreases the volume of the tumor.	– Requires consideration of combined therapies.
Wu and Qiao-dan [3]	Gradient algorithm	– It offers a rapid speed of convergence. – Reduced computational time.	– Do not include penalty terms.
Liang et al. [4]	Spearman rank correlation scheme	– Evaluates the association among SMA and p62 expressions. – Reliable approach.	– Need to analyze the association between cancer cells and CAFS.
Khalili and Ramin [5]	Steepest Descent Method	– Optimal cost function. – Personalizes the drug injection.	– Have to focus more on the closed-loop control.
Wang et al. [6]	MA	– Minimizes the tumor cells. – Improved sensitivity.	– Need to analyze the realistic diagnosis via implementation.
Nazila and Lotfi [7]	Ridge regression method	– Reduced cost. – Lessens the effort and time.	– The logical parameters have to be concentrated more.
Sofiane et al. [8]	PID controller	– Minimizes the processing time. – Better accuracy.	– Have to focus on the processing of control design.

cells where the growth is inspired by means of the tumor existence such as T-cells. It is also presumed that the entire cell populations are destroyed using a chemotherapeutic drug with varied proportions.

Bone marrow and lymph nodes are certain resources, which could develop a constant source for ID cells, st as revealed in the first term of Eq. (1). Here $\frac{\rho ID \cdot T}{T}$ specifies the saturation function with positive constraints that involve ρ and α and this constraint directly reveals that the immune cells are stimulated by tumor cells. Also $q_1 ID \cdot T$ reveals the competition among the immune and tumor cells that causes immune cell loss. Here, $y_1 u_1 ID$ denotes the immune cell loss due to the injection of drugs, and $t_1 ID$ symbolizes that the immune cells get destroyed at t_1 natural death rate.

In Eq. (2), $ra_1 T(1 - c_1 T)$ denotes the enlargement of the tumor cell population that is portrayed as the logistic term with t_1^{-1} utmost carrying capability and ra_1 growth rate. The conflicts between the growth rate and death rate are defined by the logistic growth term [26]. $q_2 ID \cdot T$ specifies the competition among immune and tumor cells, which results in tumor cell loss. Likewise, the conflicts among tumor and normal cells are defined by $q_3 TD$ which causes the tumor cell loss and $y_2 u_2 R$ refers to the tumor cell loss owing to drug injection.

In Eq. (3), the population growth of normal cells is indicated by $ra_2 D(1 - c_2 D)$ as the logistic model with ra_2 growth rate and t_2^{-1}. In addition, $y_3 u_3 D$ denotes the normal cell loss owing to drug injection, and $q_4 RD$ signifies the conflicts among normal and tumor cells that cause normal cell loss.

Modeling of robust adaptive control system

In this section, a robust adaptive control system is described for the third-order nonlinear model. Figure 1 demonstrates the schematic control structure diagram to obtain the optimal Q and R as well as optimal dosage control signal. The controller's aim is to track the states of the system (immune, tumor and normal cells) with respective optimal values. So as to achieve this objective, the volumes of biological cells (immune, tumor and normal) are evaluated over their optimal values and the error signals are produced, and the dosages of drugs are suggested as per this. In addition, for modeling a robust system over parameter uncertainty, the parameters are estimated and exploited in the control loop. The third-order model of tumor given by Eqs. (1)–(3) is rewritten as in Eq. (4), which is further rearranged in Eq. (5).

$$\begin{bmatrix} \vec{ID} \\ \vec{T} \\ \vec{D} \end{bmatrix} = \begin{bmatrix} 1\,0\,0 \\ \frac{ID \cdot T}{\alpha + T}\,0\,0 \\ -ID \cdot T\,0\,0 \\ -ID\,0\,0 \\ 0\,T\,0 \\ 0\,T^2\,0 \\ 0\,-T^2\,0 \\ 0\,-ID\,0 \\ 0\,-TD\,0 \\ 0\,0\,D \\ 0\,0\,-D^2 \\ 0\,0\,-TD \end{bmatrix}^T \begin{bmatrix} st \\ \rho \\ q_1 \\ t_1 \\ ra_1 \\ ra_1c_1 \\ q_2 \\ q_3 \\ ra_2 \\ ra_2t_2 \\ q_4 \end{bmatrix} - \begin{bmatrix} y_1IDu_1 \\ y_2Tu_2 \\ y_3Du_3 \end{bmatrix} \tag{4}$$

$$\begin{bmatrix} u_1 \\ u_2 \\ u_3 \end{bmatrix} = \begin{bmatrix} \frac{1}{T}\,0\,0 \\ \frac{T}{\alpha + T}\,0\,0 \\ -T\,0\,0 \\ -1\,0\,0 \\ \frac{-ID}{ID}\,0\,0 \\ 0\,1\,0 \\ 0\,-T\,0 \\ 0\,ID\,0 \\ 0\,-T\,0 \\ 0\,\frac{-T}{T}\,0 \\ 0\,0\,1 \\ 0\,0\,-D \\ 0\,0\,-T \\ 0\,0\,\frac{-D}{D} \end{bmatrix}^T \begin{bmatrix} \frac{st}{y_1} \\ \frac{\rho}{y_1} \\ \frac{q_1}{y_1} \\ \frac{t_1}{y_1} \\ \frac{1}{y_1} \\ \frac{ra_1}{y_2} \\ \frac{ra_1c_1}{y_2} \\ \frac{q_2}{y_2} \\ \frac{q_3}{y_2} \\ \frac{1}{y_2} \\ \frac{ra_2}{y_3} \\ \frac{ra_2c_2}{y_3} \\ \frac{q_4}{y_3} \\ \frac{1}{y_3} \end{bmatrix} \tag{5}$$

Eq.(6) portrays the regression vectors. For considering the uncertainty in the model, the constraints are substituted with the assessed values and the parameters vectors are obtained as specified in Eq. (7).

$$\begin{aligned} G_1 &= \left[\frac{1}{ID}\ \frac{T}{\alpha + T}\ -T\ -1\ \frac{-ID}{ID}\right] \\ G_2 &= \left[1\ -T\ -ID\ -D\ \frac{-T}{T}\right] \\ G_3 &= \left[1\ -D\ -T\ \frac{-D}{D}\right] \end{aligned} \tag{6}$$

$$\begin{aligned} \overline{\theta}_1 &= \left[\frac{\overline{st}}{\overline{y}_1}\ \frac{\overline{\rho}}{\overline{y}_1}\ \frac{\overline{q}_1}{\overline{y}_1}\ \frac{\overline{t}_1}{\overline{y}_1}\ \frac{1}{\overline{y}_1}\right]^T \\ \overline{\theta}_2 &= \left[\frac{\overline{ra}_1}{y_2}\ \frac{\overline{ra}_2\overline{c}_2}{y_2}\ \frac{\overline{c}_2}{\overline{y}_2}\ \frac{\overline{c}_3}{\overline{y}_2}\ \frac{1}{\overline{y}_2}\right]^T \\ \overline{\theta}_3 &= \left[\frac{\overline{ra}_2}{\overline{y}_3}\ \frac{\overline{ra}_2\overline{c}_2}{y_3}\ \frac{\overline{c}_4}{\overline{y}_3}\ \frac{1}{\overline{y}_3}\right]^T \end{aligned} \tag{7}$$

Accordingly, to formulate a stable model, the states (tumor, normal and immune cells) track their corresponding optimal values and this is derived as per Eq. (8). In Eq. (8), positive constants are denoted by γ_1, γ_2 and γ_3. ID_t and $\vec{ID}_t$ are the optimal values and the derivatives of immune cell. T_t and $\vec{T}_t$ indicates the optimal values of tumor cells and its derivatives, D_t and $\vec{D}_t$ are the desired values and its derivatives of normal cells. On substituting Eq. (8) in Eq. (6), Eq. (9) can be attained.

$$\begin{aligned} \vec{ID} &= \vec{ID}_t - \gamma_1(ID - ID_t) \\ \vec{T} &= \vec{T}_t - \gamma_2(T - T_t) \\ \vec{D} &= \vec{D}_t - \gamma_3(D - D_t) \end{aligned} \tag{8}$$

$$\begin{aligned} &G_1\left(\overline{ID}_t - \gamma_1(ID - ID_t), ID, D, T\right) \\ &\quad = \left[\frac{1}{ID}\ \frac{T}{\alpha + T} - T - 1\ \frac{-\overline{ID}_t - \gamma_1(ID - ID_t)}{IM}\right] \\ &G_2\left(\vec{T}_t - \gamma_2(T - T_t), ID, D, T\right) \\ &\quad = \left[1 - T - 1 - D\ \frac{-\vec{T}_t - \gamma_2(T - T_t)}{R}\right] \\ &G_3\left(\vec{D}_t - \gamma_3(D - D_t), ID, D, T\right) \\ &\quad = \left[1 - D - T\ \frac{-D_t - \gamma_3(D - D_t)}{D}\right] \end{aligned} \tag{9}$$

The control law in Eq. (10) is considered as per the regressor form of the system equation, in which $\overline{\theta}_1$, $\overline{\theta}_2$ and $\overline{\theta}_3$ refers to the assessing vector constraints. In addition, the adaptation law for evaluating vector parameter is given by Eq. (11), in which Γ_1, Γ_2 and Γ_3 denotes the symmetric

positive definite constant measures. The error vectors of the normal, immune, and tumor cells are signified by $\overleftrightarrow{D}$, $\overleftrightarrow{ID}$ and $\overleftrightarrow{T}$, respectively as shown in Eq. (12).

$$\begin{cases} u_1 = G_1\overline{\theta}_1 \\ u_2 = G_2\overline{\theta}_2 \\ u_3 = G_3\overline{\theta}_3 \end{cases} \tag{10}$$

$$\begin{aligned} \overline{\overline{\theta_1}} &= \overleftrightarrow{ID} \cdot ID \cdot \Gamma_1 G_1^T sign(y_1) \\ \overline{\overline{\theta_2}} &= \overleftrightarrow{T} \cdot T \cdot \Gamma_2 G_2^T sign(y_2) \\ \overline{\overline{\theta_3}} &= \overline{\overline{D}} \cdot D \cdot \Gamma_3 G_3^T sign(y_3) \end{aligned} \tag{11}$$

$$\overleftrightarrow{ID} = ID - ID_t \tag{12}$$

Enhanced Kalman filter with improved nonlinear kernel-based error function with scaling factor

The measurement of immune cells is complex in the lab environment and it also needs certain experiments and therefore a nonlinear observer is required for assessing the immune cells. In this research work, an EKF is exploited with improved nonlinear kernel-based error function with scalar function, and the processing steps are as follows.

In the initial stage, a discrete-time nonlinear system is formulated as shown in Eq. (13), in which z_k and w_k refers to the measurement and process noise, correspondingly. Here, z_k and w_k are fixed as zero-mean white Gaussian noise together with two covariance measures denoted by R and Q, as specified in Eq. (14). In Eq. (14),b_k specifies the measurement vector, which includes normal and tumor cells and a_k denotes the system states like the count of the tumor, immune, and normal cells. These vectors are portrayed by Eq. (15).

$$\begin{aligned} b_k &= f(b_{k-1}, u_{k-1}) + w_k \\ a_k &= Ub_k + z_k \end{aligned} \tag{13}$$

$$\begin{aligned} &\left\{w_k w_j^T\right\} = Q\delta_{kj} \quad Q > 0, \\ &\left\{z_k z_j^T\right\} = R\delta_{kj} \quad R > 0 \\ &\left\{w_k z_j^T\right\} = 0 \end{aligned} \tag{14}$$

$$\begin{aligned} b_k &= [ID_k \quad T_k \quad D_k]^T \\ a_k &= [T_k \quad D_k]^R \end{aligned} \tag{15}$$

The cancer chemotherapeutic model obtains$f$ as per the Eqs. (1)–(3). Eq. (11) includes assessment parameter values that are deployed in the ,' observer. Therefore, f is determined as in Eq. (16).

$$f = \begin{bmatrix} \overline{st} + \dfrac{\overline{\rho} ID_k T_k}{\overline{\alpha} + T_k} - \overline{q}_1 ID_k T_k - \overline{t}_1 ID_k - \vec{y}_1 u_{1k} ID_k \\ \overline{ra}_1 T_k (1 - \overline{c}_1 T_k) - \overline{q}_2 ID_k T_k - \overline{q}_3 T_k D_k - \vec{y}_2 u_{2k} T_k \\ \overline{ra}_2 D_k (1 - \overline{c}_2 D_k) - \overline{q}_4 T_k D_k - \vec{y}_3 u_{3k} D_k \end{bmatrix} \tag{16}$$

This EKF estimates various states by following two phases (i) prediction (ii) update.

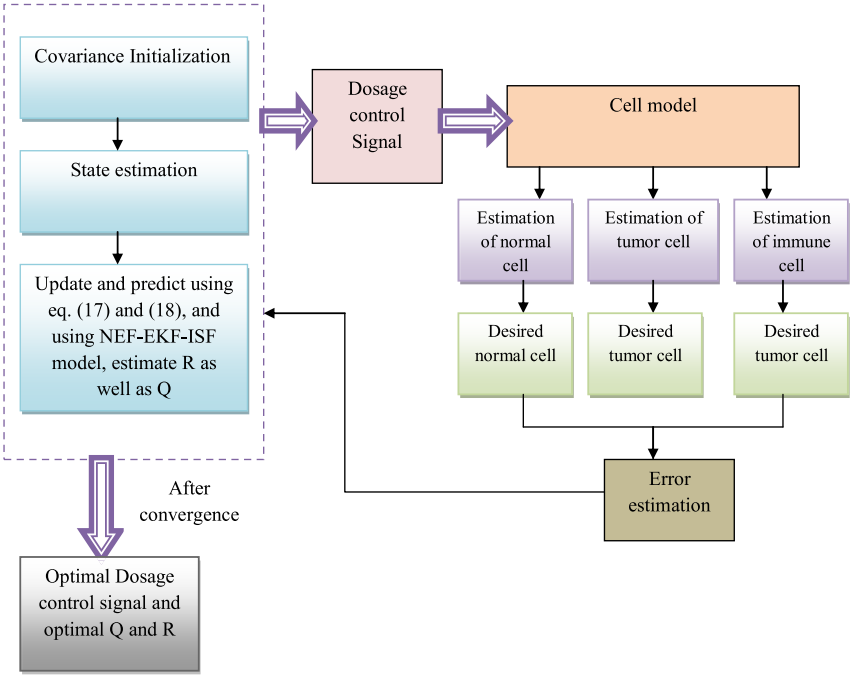

Figure 1: Block diagram of control structure.

Prediction: Eq. (17) determines the one-step prediction of $\vec{b}_{k|k-1}$ and the corresponding error covariance matrix $PR_{k|k-1}$.

Update: Here, thePR_k assessment and $\vec{b}_k$ state estimation is performed as shown in Eq. (18), in which Kalman gain is denoted byk_k. Thus, the immune cell is determined by Eqs. (17) and (18), correspondingly.

$$\vec{b}_{k|k-1} = f\left(\vec{b}_{k-1}\right)$$
$$PR_{k|k-1} = E_k PR_{k-1} E_k^T + Q_k \tag{17}$$
$$E_k = \frac{\partial f(b)}{\partial b}\Big|_{b=\vec{b}_{k-1}}$$

$$\vec{b}_k = \vec{b}_{k|k-1} + k_k\left(a_k - U_k \vec{b}_{k|k-1}\right)$$
$$k_k = PR_{k|k-1} U_k^T \left(U_k PR_{k|k-1} U_k^T + R_k\right)^{-1} \tag{18}$$
$$PR_k = \left(PR_{k|k-1}^{-1} + U_k^T R_k^{-1} U_k\right)^{-1}$$

Improved nonlinear kernel-based error function with new scaling factor for covariance matrix estimation

The Kalman filter's performance is entirely based on "how the user chooses the exact Q_k and R_k for various applications". As per the existing scheme, R_k and Q_k are fixed as the constant matrix that is attained by trial and error approach. However, problems arise during the selection process, and hence to enhance the performance, in [28] their introduces a novel covariance matrix estimation under the nonlinear kernel-based error function. Subsequently, this research work intends to make a specified enhancement with the existing error function by introducing a new scaling factor. Here, in [27] the estimation schemes are classified into varied means, in which the covariance matching is regarded as the well-known approach for estimation. The scheme tunes the covariance matrix of residual or innovation depending on the theoretical values. While predicting the EKF, the innovation is the variation amongst the actual and predicted measurement, while the residual is the variation amongst actual and estimated measurement. This error measure at step$k(\varepsilon_k)$ is portrayed by Eq. (19), in which o_k indicates the measurement function, h_k and $\vec{b}_k^+$ refers to the actual and estimated value. For attaining better performance, an enhancement is done with the error measure computation, where the differential evaluation of error measure $\partial\varepsilon_k$ is computed as specified in Eq. (20).

$$\varepsilon_k = \left[h_k - o_k\left(\vec{b}_k^+\right)\right] \tag{19}$$

$$\partial\varepsilon_k = \exp\left(\frac{\varepsilon_k}{\varepsilon_k^-}\right) \cdot \varepsilon_k \tag{20}$$

Residual-based improved estimation of *R*

The R_k estimation depending on innovation is indicated by Eq. (21), in which the covariance matrix of innovation is specified by H_k. In this context, R_k should be a positive definite matrix; however, this is not the case as per Eq. (21), as R_k is computed by performing the subtraction of 2 positive definite matrixes. For ensuring the positive definite matrix, the adopted enhanced ESK model estimates the R_k under $\partial\varepsilon_k$ as shown by Eq. (20). This novel R_k estimation is given by Eq. (23), in which b shows the count of system states and in Eq. (22), V refers to the defined improvement factor.

$$R_k = H_k - U_k^{[1]} PR_k^- U_k^{[1]T} \tag{21}$$

$$V = R_{k-1} + \left(\partial\varepsilon_k \partial\varepsilon_k^T + U_k^{[1]} PR_k^- U_k^{[1]T}\right) \tag{22}$$

$$R_k = \frac{\log(V)}{b} \tag{23}$$

In the conventional methods [27], the error is calculated using the traditional difference function and it is used for the updating process of the EKF. In our previous work [28], it has been changed to the nonlinear error function. Here, the updating process relies on the previous error function, though scaled to a nonlinear environment. It is obvious that the updating process should rely on historical error improvements. Hence, in this research work, introduces a scaling factor, which considers the historical error improvement, for the updating process. Since the error improvement at the n-1th instant is more significant than the 2nd instant, appropriate weightage for the instantaneous error improvement is important. By considering this factor, we have formulated a scaling factor for updating the principle that enables the updating process as coarse-grained and fine-tuned. The formulation of improvement factor$V$ with the new scaling factor is given by Eq. (24), where, SF denotes the proposed scaling factor.

$$V = R_{k-1} + \left(\partial\varepsilon_k \partial\varepsilon_k^T + U_k^{[1]} PR_k^- U_k^{[1]T}\right) \times [SF] \tag{24}$$

The scaling factor SF can be computed as per Eq. (25), where, σe denotes the standard deviation, n refers to the number of instants and we specifies the weight. Here, we is computed as per Eq. (26), where In denotes the previous instants together with the current instants and CIn refers to

the current instants.Here σe is computed as per Eq. (27), where nu refers to the number of data points, x_i denotes each value of data and $\overline{x}$ indicates the mean of x_i. The computation model of the considered parameters of SF is given by Table 2 (exemplary table).

$$SF = \frac{\sigma e}{n} \sum_{i=1}^{n} we_i \tag{25}$$

$$we = \frac{In}{CIn} \tag{26}$$

$$\sigma e = \sqrt{\sum_{i=1}^{nu} \frac{(x_i - \overline{x})^2}{nu - 1}} \tag{27}$$

Innovation-based estimation of *Q*

The process noise is computed as in Eq. (28) for estimating the Q_{k-1}. The average evaluation of Q with respect to time is portrayed by Eq. (29), in which k_k denotes the Kalman gain and α denotes the forgetting factor (fixed as 0.3 as per [27]). The overall contribution of adopted control theory by deploying enhanced Kalman filter is given by Figure 2.

$$w_{k-1} = b_k - \Phi(b_{k-1}, u_{k-1}) \tag{28}$$

$$Q_k = \alpha Q_{k-1} + (1 - \alpha)\left(k_k t_k t_k^T k_k^T\right) \tag{29}$$

The EKF model differs from the conventional EKF model in estimating the R by using a novel scaling factor. The scaling factor transforms the estimated R value to a new updating process so that the next state error can be significantly minimized.

Results and discussion

Simulation procedure

The presented control theory for cancer chemotherapy was implemented in MATLAB 2018 a. Here, the analysis was carried out by setting the nominal constraints of chemotherapy as demonstrated in Table 2. Further, the performance of the presented NEF-EKF-ISF control model was compared over other existing approaches such as EKF [10], AEKF [27] and NEF-EKF [28] and the outcomes have confirmed the efficiency of NEF-EKF-ISF in controlling the states (immune, normal and tumor cells). "In statistics, the MSE or MSD of an estimator (of a procedure for estimating an unobserved quantity) measures the average of the squares of the errors—that is, the average squared difference between the estimated values and the actual value. It is always non-negative, and values closer to zero are better".

Table 2: Computation of the scaling factor.

Number of instants *n*	Error computation Δ*e*	Standard deviation *σe*	Weight factor *we*
Σe	Weight factor (we)		
1	–	–	–
2	$e_1 - e_0$	σe_1	$\frac{1}{2} + \frac{2}{2}$
3	$e_2 - e_1$	σe_2	$\frac{1}{3} + \frac{2}{3} + \frac{3}{3}$
⋮	⋮	⋮	⋮
n	$e_{n-1} - e_{n-2}$	σe_n	$\frac{1}{n} + \frac{2}{n} + \frac{3}{n} + ... + \frac{n}{n}$

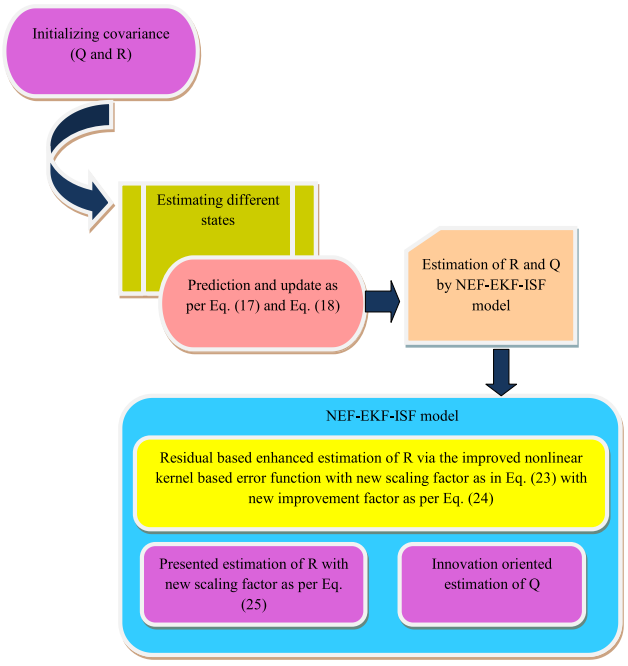

Figure 2: Diagrammatic representation of proposed model.

3-D analysis

The impact of the adopted control theory (NEF-EKF-ISF) on controlling three states (normal, immune and tumor cells) is demonstrated by Figure 3. The objective of this control theory is to determine the dosage of drugs, which could completely destroy the tumor cells. The attained results show the demonstration of how much the presented approach comes closer to eliminating the tumor cells.

Convergence analysis

Figure 4 shows the time response of the entire states attained by the system. The addressed values are the

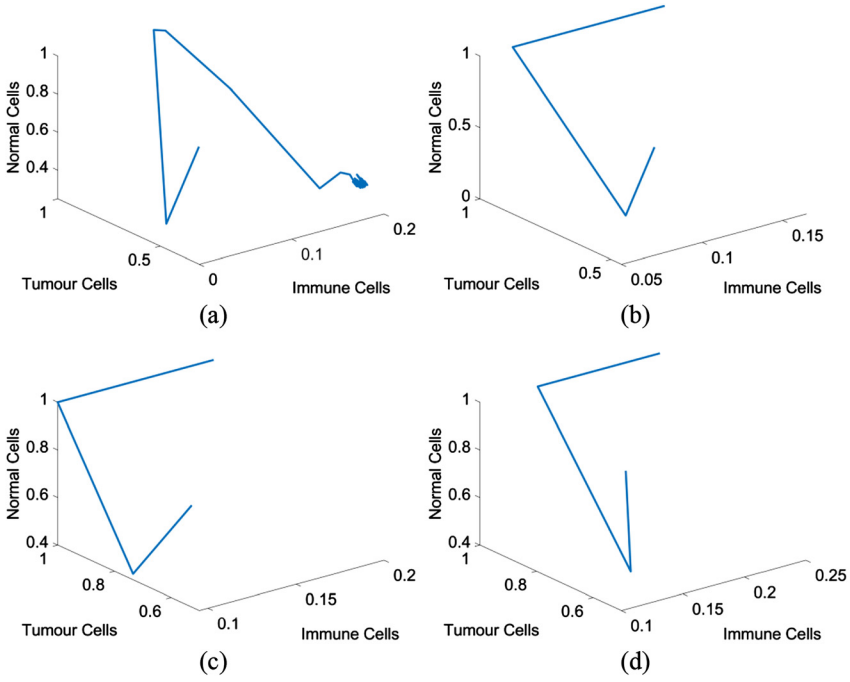

Figure 3: 3D analysis on the impact of proposed and conventional control theory (a)EKF (b) AEKF (c) NEF-EKF (d) NEF-EKF-ISF.

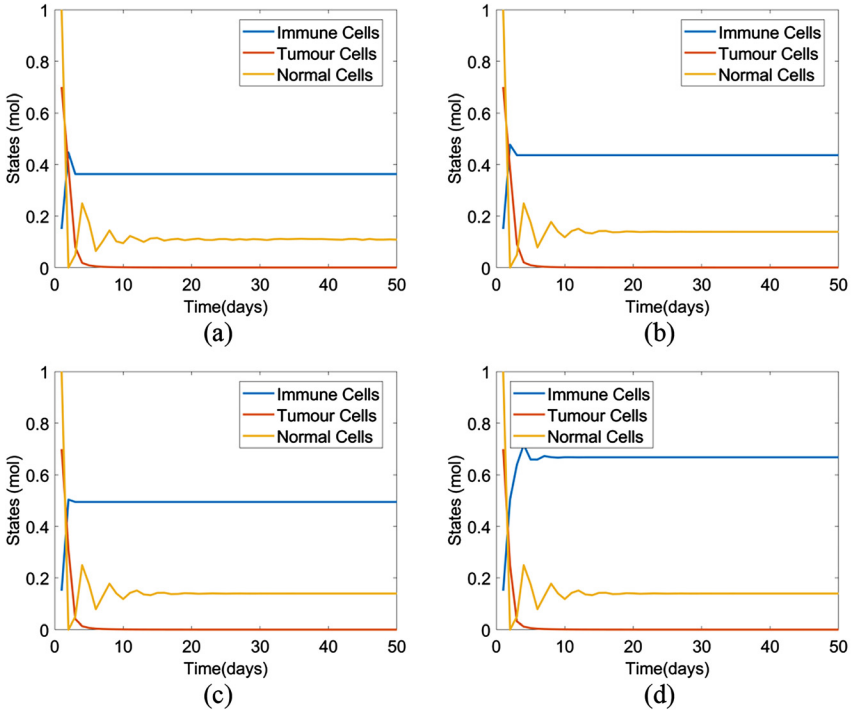

Figure 4: Convergence analysis (a) EKF (b) AEKF (c) NEF-EKF(d) NEF-EKF-ISF

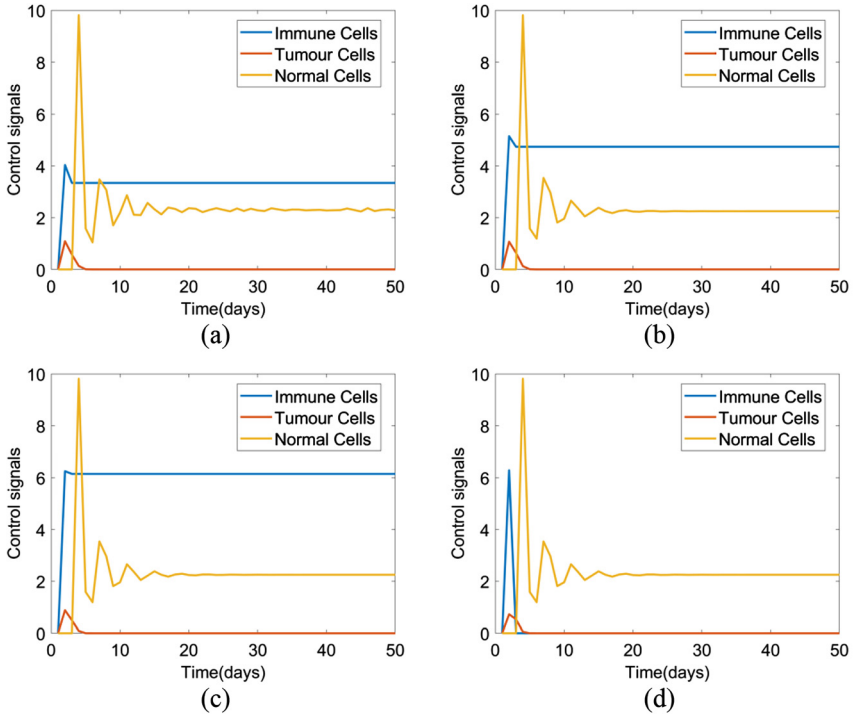

Figure 5: Control Signals under chemotherapy drug dosage (a) EKF (b) AEKF (c) NEF-EKF (d) NEF-EKF-ISF.

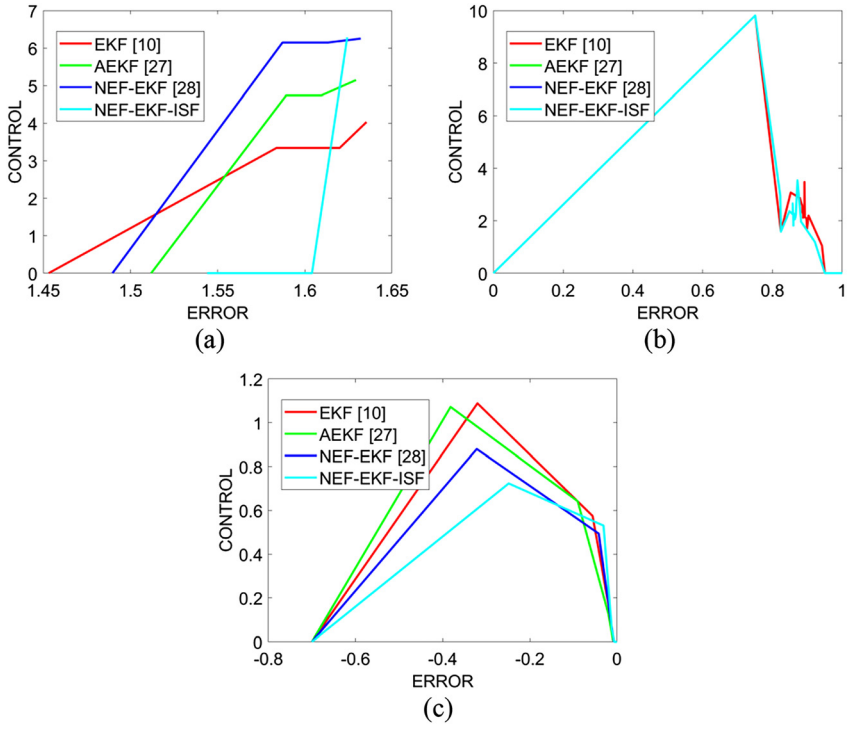

Figure 6: Response of control signals for error signal variation : Proposed and conventional control theories under chemotherapy drug dosage (a) immune (b) normal (c) tumor.

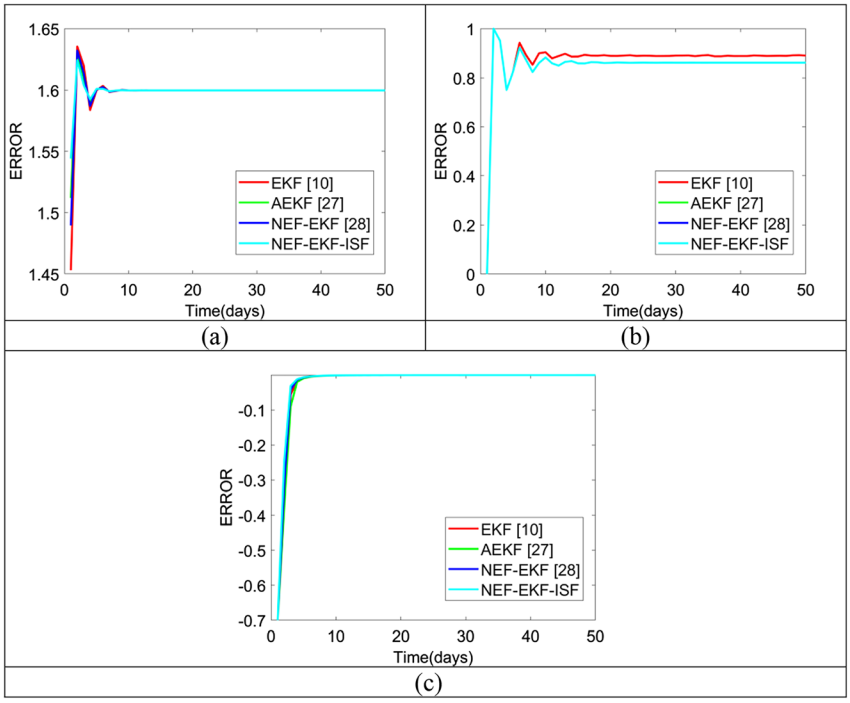

Figure 7: Time analysis: proposed and conventional control models under chemotherapy drug dosage (a) immune (b) normal (c) tumor.

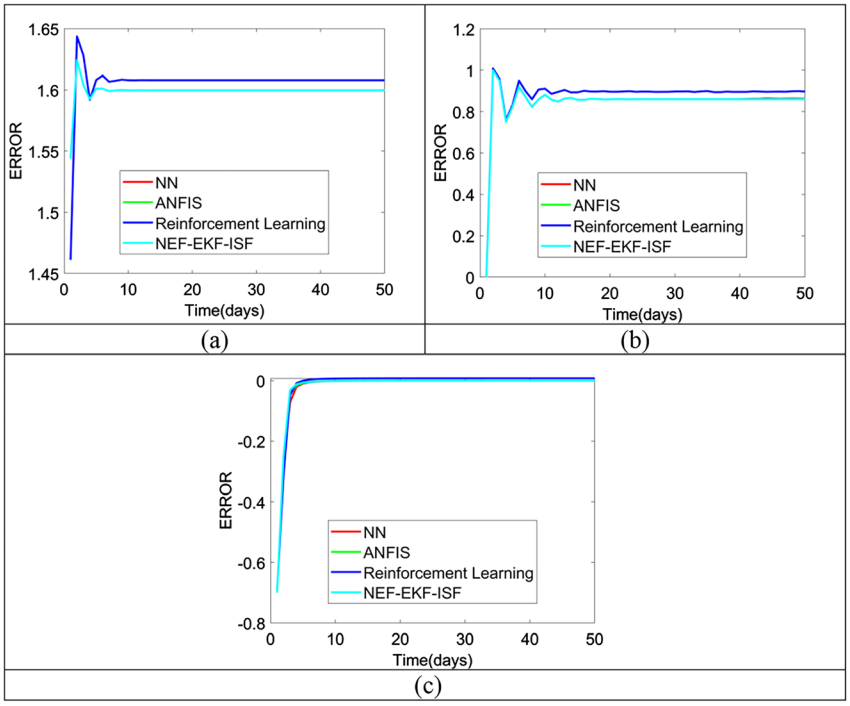

Figure 8: Error analysis: proposed and conventional control models under chemotherapy drug dosage (a) Immune (b) Normal (c) Tumor.

Table 3: Nominal chemotherapy parameters.

Parameter	Value
y_1	0.05
y_2	**0.15**
y_3	0.1
ra_1	1.5
ra_2	1.0
t_1	0.2
q_1	1.0
q_2	0.5
q_3	1.0
q_4	1.0
c_1^{-1}	1.0
c_2^{-2}	1.0
st	0.33
α	0.3
ρ	0.01

estimated values, that when utilized in the controllers, the states could track their corresponding optimal values. From Figure 4 (d), the tracking of desired values particularly the tumor cells depicts that the presented work is stable in the existence of a modeled observer. Thus, the implemented NEF-EKF-ISF observer attains better outcomes by tracking the desired values of the state.

Convergence analysis of injecting drug dosage

The graphical illustration of the chemotherapy drug dosages u_1, u_2 and u_3 that converges the normal, immune and tumor cells to their corresponding desired values is given in Figure 5. Since the major intention of this work relies on converging the values to the optimal values, the presented scheme attempts to converge by providing control signals to the entire states. Figure 5(d) shows the betterment of the adopted model in attaining the desired values.

Error analysis

This section explains the error performance with respect to the control signals for three states namely, normal, immune and tumor cells. From the attained outputs, the presented method has attained a reduced error value over the other conventional schemes. From Figure 6(c), at −0.4th error value, the control signal value of the adopted scheme is 60%, 80% and 20% better than EKF, AEKF and NEF-EKF approach. Thus, the enhancement of the adopted scheme is proved from the simulation outcomes.

Time analysis

Figure 7 demonstrates the occurrence of error for the presented method over the traditional approaches with respect to the time represented in days. From the analysis, the reduced error value is achieved by the presented scheme with an increase in time, when evaluated over the conventional schemes.

Error analysis

Figure 8 demonstrates the occurrence of error for the developed algorithm over the existing algorithms concerning the time represented in days. From the analysis, the error value is reduced by the developed model with an increase in time, when evaluated over the conventional schemes.

Overall performance

The overall performance of the presented scheme over other existing approaches on tracking the desired values of the states (immune, normal and tumor) is demonstrated in Table 4. From the analysis, the proposed control theory is found to have attained the closest desired values over the other compared models such as EKF [10], AEKF [27], NEF-EKF [28], NN [34], ANFIS [35] and reinforcement learning [36]. In addition, the least estimated values are obtained by the tumor cells, which also indicate the non-existence of the tumor cells. Therefore, better parameter estimation is proved to be attained by the presented

Table 4: Overall performance of proposed control theory over other conventional theories.

	EKF [10]	AEKF [27]	NEF-EKF [28]	NN [34]	ANFIS [35]	Reinforcement learning [36]	NEF-EKF-ISF
Immune cells (mol)	1.3394	1.2686	1.2119	1.0453	1.0453	1.3274	1.0453
Tumor cells (mol)	0.024439	0.02461	0.021895	0.021542	0.020884	0.036439	0.020437
Normal cells (mol)	0.87244	0.84626	0.84626	0.84675	0.84627	0.88192	0.84626

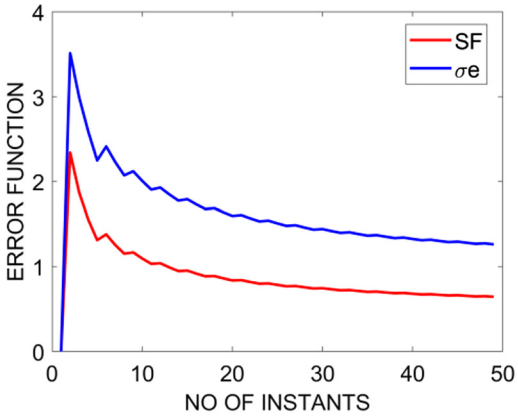

Figure 9: Analysis of error function with respect to the number of instants.

NEF-EKF-ISF model over the other conventional approaches.

Analysis of error function

The analysis of the error function is illustrated by Figure 9 with respect to the number of instants. Here the error function of the scaling factor *SF* and standard deviation σe are computed, which demonstrates the decrement of the error value with an increase in the number of instants. Thus, the enhancement of the updating process is proved to be better using the presented NEF-EKF-ISF scheme.

Conclusion

This paper has presented a novel robust controller that influences the drug dosage together with parameter estimation. Here, a novel NEF-EKF-ISF was introduced and the updating process was done depending on the prior error function, though scaled to a nonlinear environment. Further, a scaling factor was established that considered the historical error enhancement for the updating process. Finally, the performance of the implemented controller was compared over other traditional schemes that demonstrate the impact of drug dosage injection on normal, immune and tumor cells. On considering the time response of the entire states, the tracking of desired values particularly the tumor cells was found to be stable in the existence of modeled observer as per the presented work. Further, at −0.4th error value, the control signal value of the adopted scheme was 60, 80, and 20% better than EKF, AEKF, and NEF-EKF approach. Thus, the parameter value estimation of the implemented NEF-EKF-ISF approach in attaining the desired values of system states was confirmed.

Research funding: None declared.
Author contributions: All the authors have accepted responsibility for the entire content of this submitted manuscript and approved submission.
Conflict of interest: The authors declare that they have no conflict of interest.
Informed consent: Informed consent was obtained from all individuals included in this study.
Ethical approval: The conducted research is not related to either human or animal use.

References

1. Padmanabhan R, Meskin N, Haddad WM. Reinforcement learning-based control of drug dosing for cancer chemotherapy treatment. Math Biosci 2017;293:11–20.
2. Lai X, Friedman A. Mathematical modeling in scheduling cancer treatment with combination of VEGF inhibitor and chemotherapy drugs. J Theor Biol 2019;462:490–8.
3. Wu X, Liu Q, Zhang K, Cheng M, Xin X. Optimal switching control for drug therapy process in cancer chemotherapy. Eur J Contr 2018;42:49–58.
4. Liang L, Luo H, He Q, You Y, Liang J. Investigation of cancer-associated fibroblasts and p62 expression in oral cancer before and after chemotherapy. J Cranio-Maxillofacial Surg 2018;46: 605–10.
5. Khalili P, Vatankhah R. Derivation of an optimal trajectory and nonlinear adaptive controller design for drug delivery in cancerous tumor chemotherapy. Comput Biol Med 2019;109: 195–206.
6. Wang P, Liu R, Jiang Z, Yao Y, Shen Z. The optimization of combination chemotherapy schedules in the presence of drug resistance. IEEE Trans Autom Sci Eng 2019;16:165–79.
7. Bazrafshan N, Lotfi MM. A multi-objective multi-drug model for cancer chemotherapy treatment planning: a cost-effective approach to designing clinical trials. Comput Chem Eng 2016;87: 226–33.
8. Khadraoui S, Harrou F, Nounou HN, Nounou MN, Bhattacharyya SP. A measurement-based control design approach for efficient cancer chemotherapy. Inf Sci 2016;333:108–25.
9. Batmani Y, Khaloozadeh H. Optimal drug regimens in cancer chemotherapy: a multi-objective approach. Comput Biol Med 2013;43:2089–95.
10. Rokhforoz P, Jamshidi AA, Sarvestani NN. Adaptive robust control of cancer chemotherapy with extended Kalman filter observer. Inf Med Unlocked 2017;8:1–7.
11. Chen T, Kirkby NF, Jena R. Optimal dosing of cancer chemotherapy using model predictive control and moving horizon state/ parameter estimation. Comput Methods Progr Biomed 2012;108: 973–83.
12. Paryad-zanjani S, Mahjoob MJ, Amanpour S, Kheirbakhsh R, Akhoundzadeh MH. A supplemental treatment for chemotherapy: control simulation using a mathematical model with estimated

parameters based on in vivo experiment. IFAC-Papers OnLine 2016;49:277–82.
13. Pouchol C, Clairambault J, Alexander L, Trélat E. Asymptotic analysis and optimal control of an integro-differential system modelling healthy and cancer cells exposed to chemotherapy. J Math Pure Appl 2018;116:268–308.
14. Matsuda C, Ishiguro M, Teramukai S, Kajiwara Y, Fujii S, Kinugasa Y, et al. A randomised-controlled trial of 1-year adjuvant chemotherapy with oral tegafur–uracil versus surgery alone in stage II colon cancer: SACURA trial. European Journal of Cancer 2018;96:54–63.
15. Toyooka S, Okumura N, Nakamura H, Nakata M, Yamashita M, Tada H, et al. A multicenter randomized controlled study of paclitaxel plus carboplatin versus oral uracil-tegafur as the adjuvant chemotherapy in resected non–small cell lung cancer. J Thorac Oncol 2018;13:699–706.
16. Wu H, Hu H, Wan J, Li Y, Wu Y, Tang Y, et al. Hydroxyethyl starch stabilized polydopamine nanoparticles for cancer chemotherapy. Chem Eng J 2018;349:129–45.
17. Gibbons A, Groarke AM. Coping with chemotherapy for breast cancer: asking women what works. Eur J Oncol Nurs 2018;35: 85–91.
18. Jiang S, Liu Y, Huang L, Zhang F, Kang R. Effects of propofol on cancer development and chemotherapy: potential mechanisms. Eur J Pharmacol 2018;831:46–51.
19. Sun B, Luo C, Cui W, Sun J, He Z. Chemotherapy agent-unsaturated fatty acid prodrugs and prodrug-nanoplatforms for cancer chemotherapy. J Contr Release 2017;264:145–59.
20. Wang F, Porter M, Konstantopoulos A, Zhang P, Cui H. Preclinical development of drug delivery systems for paclitaxel-based cancer chemotherapy. J Contr Release 2017; 267:100–18.
21. Abbasian M, Roudi MM, Mahmoodzadeh F, Eskandani M, Jaymand M. Chitosan-grafted-poly(methacrylic acid)/graphene oxide nanocomposite as a pH-responsive de novo cancer chemotherapy nanosystem. Int J Biol Macromol 2018;118:1871–9. Available online.
22. Bao T, Seidman AD, Piulson L, Vertosick E, Chen X, Vickers AJ, et al. A phase IIA trial of acupuncture to reduce chemotherapy-induced peripheral neuropathy severity during neoadjuvant or adjuvant weekly paclitaxel chemotherapy in breast cancer patients. Eur J Canc 2018;101:12–19.
23. Gretchen, Kimmick G, Li X, Fleming ST, Sabatino SA, Wilson JF, et al. Risk of cancer death by comorbidity severity and use of adjuvant chemotherapy among women with locoregional breast cancer. J Geriatric Oncol 2018;9:214–20.
24. Kurt B, Kapucu S. The effect of relaxation exercises on symptom severity in patients with breast cancer undergoing adjuvant chemotherapy: an open label non-randomized controlled clinical trial. Eur J Integr Med 2018;22:54–61. Available online.
25. Sun X, Zhang M, Du R, Zheng X, Tang C, Wu Y, et al. A polyethyleneimine-driven self-assembled nanoplatform for fluorescence and MR dual-mode imaging guided cancer chemotherapy. Chem Eng J 2018;350:69–78.
26. Schattler H, Ledzewicz U. Optimal control for mathematical models of cancer therapies. Springer; 2010.
27. Akhlaghi S, Zhou N, Huang Z. Adaptive adjustment of noise covariance in kalman filter for dynamic state estimation. Syst Contr 2017. https://doi.org/10.1109/PESGM.2017.8273755.
28. Utkarsha. Non-linear kernel-based error function for extended kalman filter oriented robust control of cancer chemotherapy. In communication.
29. Nasiri H, Kalat AA. Adaptive fuzzy back-stepping control of drug dosage regimen in cancer treatment. Biomed Signal Process Contr 2018;42:267–76.
30. Sharifi M, Moradi H. Nonlinear composite adaptive control of cancer chemotherapy with online identification of uncertain parameters. Biomed Signal Process Contr 2019;49:360–74.
31. Teles FF, Lemos JM. Cancer therapy optimization based on multiple model adaptive control. Biomed Signal Process Contr 2019;48:255–64.
32. Zouari F, Ibeas A, Boulkroune A, Cao J, Arefi MM. Neuro-adaptive tracking control of non-integer order systems with input nonlinearities and time-varying output constraints. Inf Sci 2019; 485:170–99.
33. Zouari F. Neural network based adaptive backstepping dynamic surface control of drug dosage regimens in cancer treatment. Neurocomputing 2019;366:248–63.
34. Xuan W, You G. Detection and diagnosis of pancreatic tumor using deep learning-based hierarchical convolutional neural network on the internet of medical things platform. Future Generat Comput Syst 2020;111:132–42.
35. Selvapandian A, Manivannan K. Fusion based Glioma brain tumor detection and segmentation using ANFIS classification. Comput Methods Progr Biomed 2018;166:33–8.
36. Yazdjerdi P, Meskin N, Al-Naemi M, Moustafa A-EA, Kovács L. Reinforcement learning-based control of tumor growth under anti-angiogenic therapy. Comput Methods Progr Biomed 2019; 17:15–26.
37. Beno MM, Rajakumar BR. Threshold prediction for segmenting tumour from brain MRI scans. Int J Imag Syst Technol 2014;24: 129–37.
38. Fedele L. Design of organization and safety measures for the reclamation from friable asbestos of an industrial area in Italy; 2016.
39. Jameel AS, Ahmad AR. The mediating role of job satisfaction between leadership style and performance of academic staff. Int J Psychosoc Rehabil 2020;24:2399–414.
40. Cofini V, Carbonelli A, Cecilia MR, Di Orio, F. Quality of life, psychological wellbeing and resilience: a survey on the Italian population living in a new lodging after the earthquake of April 2009. 2014;26:46–51.
41. Bonacaro A, Rubbi I, Sookhoo D. The use of wearable devices in preventing hospital readmission and in improving the quality of life of chronic patients in the homecare setting: a narrative literature review. Professioni infermieristiche 2019;72.
42. Bonacaro A, Morgan L. Simulated mindfulness meditation: a major breakthrough in the management of chronic pain, 2016.